

Received January 10, 2020, accepted January 28, 2020, date of publication February 3, 2020, date of current version February 12, 2020.

Digital Object Identifier 10.1109/ACCESS.2020.2971316

Realization of Electrically Small, Low-Profile Quasi-Isotropic Antenna Using 3D Printing Technology

SONAPREETHA MOHAN RADHA¹, (Student Member, IEEE),
GEONYEONG SHIN¹, (Student Member, IEEE),
PANGUN PARK², (Member, IEEE), AND
ICK-JAE YOON¹, (Member, IEEE)

¹Department of Electrical Engineering, Chungnam National University, Daejeon 34134, South Korea

²Department of Radio and Information Communications Engineering, Chungnam National University, Daejeon 34134, South Korea

Corresponding author: Ick-Jae Yoon (ijyoon@cnu.ac.kr)


This work was supported in part by the Basic Science Research Program of the National Research Foundation of Korea funded by the Ministry of Science, ICT, and Future Planning, under Grant NRF-2019R1F1A1063474, and in part by the Basic Research Laboratory of the National Research Foundation funded by the Korean Government under Grant NRF-2017R1A4A1015744.

ABSTRACT A 3D printed, low-profile, electrically small antenna with a quasi-isotropic radiation pattern is presented herein. It is composed of an electric meandered dipole antenna, and the extended arcs from the meander line mimicking the current flow of the loop antenna. A quasi-isotropic radiation pattern is achieved from the total current flow over the proposed structure. Modern stereolithographic 3D printing and nano-polycrystalline copper coating technologies are used to build a prototype. The measured antenna exhibits a good uniformity in terms of the radiation pattern with a maximum gain deviation of 4.5 dB at 959 MHz and a radiation efficiency of 81 %, close to the computed expectations. The electrical size of the antenna ka is 0.48, and its height is $\lambda_0/82.32$.

INDEX TERMS 3D printing, isotropic radiation pattern, electrically small antennas, radiation pattern synthesis.

I. INTRODUCTION

Research on the realization of an isotropic antenna is demanding due to its characteristic of uniform wireless signal reception. This type of antenna could be effectively used in various applications, including RFID systems, aerospace, energy harvesting and industrial equipment. Despite the huge demand for this type of antenna, however, the theoretical work has found that an antenna with a perfect isotropic radiation pattern does not exist in practice [1]. Nevertheless, intensive studies have been conducted to achieve a nearly isotropic radiation pattern, which is also often referred to as a quasi-isotropic radiation pattern. A common strategy to achieve a quasi-isotropic radiation pattern is to bring electric and magnetic dipoles together perpendicularly, such that the null-field direction of one dipole is along the maximum-field direction

The associate editor coordinating the review of this manuscript and approving it for publication was Kai Lu .

of the other dipole, minimizing the blind spots of each dipole. Several associated designs have been reported [2]–[8]. In [2], a split-ring resonator was folded, such that both the current distributions of electric and magnetic dipoles can be formed simultaneously. Further, a monopole antenna was properly wrapped on a 3D-printed package in [3], showing the quasi-isotropic radiation pattern at dual frequency bands, and inductively coupled meander line structures were folded around the sides of a cube in [4]. The proposed antennas in [2]–[4] occupy a three-dimensional space. A planar type quasi-isotropic antenna is also feasible using the same technique of radiation pattern synthesis of electric and magnetic dipoles [5]–[7] or two crossed electric dipoles [8]. Although many of the reported quasi-isotropic antennas are electrically small, they are not necessarily small. An antenna with an electrical size of $ka > 1.0$ could also show the desired pattern at a relatively larger frequency bandwidth than the antenna with $ka < 0.5$. ka is one of the most commonly used parameters to

measure the electrical size of antennas, where k is the free-space wave propagation constant and a is the radius of the imaginary sphere enclosing the antenna.

An antenna is usually said to be electrically small when ka is less than 0.5. Electrically small antennas (ESAs) are essential in modern wireless technology since the space allotted for antenna installation in electronic and mobile devices has become smaller. The study of ESAs has a long history, and various miniaturization techniques exist [9]–[15]. Most of them are related to changing the electrical and physical configurations of the antenna as a means of reducing the resonant frequency with acceptable radiation properties. Thus, highly efficient ESAs could take a complex three-dimensional shape, and some trials utilize 3D-printing (3DP) technologies for the easier and faster prototyping of novel and complex antenna designs [16]–[21]. 3DP technology can print an object from a CAD model with an enormous amount of design freedom and is widely used in the various fields such as agriculture, electronics, healthcare, automotive industry, only to mention a few. However, despite its recent explosive growth in scientific applications, it is not yet well suited for very small designs, and not all geometries can be finely built with sufficient conductivity using the commercially available 3DP technologies at their present technology level [22].

In this paper, we propose a novel low-profile design of a self-resonant ESA with a high radiation efficiency and a good quasi-isotropic radiation pattern. It is designed and tested at the 900 MHz ISM frequency band. Stereolithography (SLA) 3DP and nano-polycrystalline copper coating methods are used in its experimental validation. The measured impedance and radiation properties of the prototype show good agreement with the computed expectations. We use HFSS from Ansys for the full-wave electromagnetic simulations in this work.

II. ANTENNA DESIGN

The proposed design concept is illustrated in Fig. 1. It is composed of an electrically small dipole at the center and an electrically small loop circulating it, made of extended lines from both the open ends of the electric dipole arranged in clockwise and counterclockwise directions. One arm of the dipole is positioned slightly up and the other arm is positioned slightly down with respect to the xy -plane to alleviate any possible physical overlap. The structure is fed by a single port

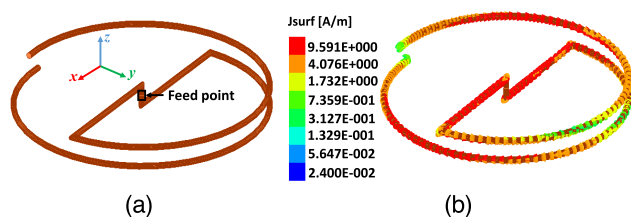


FIGURE 1. Design concept. (a) Electric dipole at the center and a loop-like configuration surrounding it. (b) Current distribution.

at the center of the electric dipole. Fig. 1b shows that a nearly uniform current distribution can be formed on each part of the electric dipole and loop with an electrically small dimension (dipole length = 0.1λ). In Section 2.A, it is stated whether this design concept can be realized with proper impedance and radiation properties. Next, in Section 2.B, it is stated how the proposed complex design is physically tuned so that it could be properly built using 3DP and nano-polycrystalline technologies, while maintaining the electrical properties.

A. ANTENNA CONFIGURATION AND FEASIBILITY CHECK

The conceptual design in Fig. 1 now adopts a meander line to increase the electrical length of the antenna, as shown in Fig. 2. The extended line from one end of the meander line ($z > 0$) works similarly to a top-loading structure of a top loaded monopole antenna [23], since it creates an extra current flow path and eventually makes the antenna self-resonant with a sufficient radiation resistance close to a $50\text{-}\Omega$. It also forms a loop configuration together with the bottom part at the opposite side ($z < 0$). With the length of the loop ($\alpha = 271.28^\circ$), the radius of the loop ($r = 24\text{ mm}$), and the gap between the top and bottom parts ($g = 0.2\text{ mm}$), one can obtain the desired radiation properties at the 900 MHz-ISM frequency band. The antenna structure is made of a copper strip ($h = 0.8\text{ mm}$, $t = 1.6\text{ mm}$) and is fed at the center of the

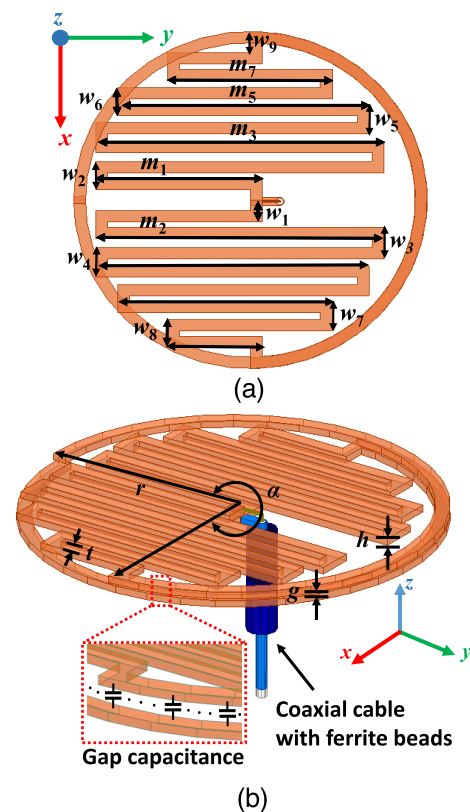


FIGURE 2. Antenna configuration with the design parameters of the proposed antenna. (a) Top view. (b) Birds view.

meander dipole using a coaxial cable. The inner conductor of the cable is connected to the top part ($z > 0$), whereas the outer conductor is connected to the bottom part ($z < 0$). The electrical properties of a ferrite bead are characterized and placed at the outer conductor of the cable in the full-wave electromagnetic simulation to prevent the current from flowing through the outer jacket of the cable, which would affect the radiation pattern.

The designed antenna in Fig. 2 is self-resonant at 915 MHz. Other simulated results are shown in Fig. 3. The peak gain and radiation efficiency across the frequency are given in Fig. 3a. The maximum gain deviation over the entire space is 2.86 dB, as shown in Fig. 3b, which is good enough to be considered as an antenna with a quasi-isotropic radiation pattern. The simulated radiation efficiency at 915 MHz is 89.8% with ka of 0.47. Due to its complex structure, the above-mentioned simulated design was tried to be fabricated using a selective laser sintering (SLS) 3D printer with a polyamide material of PA2200. However, then it was found that metallization over a $g = 0.2$ mm gap is challenging since the metal paste needs to be painted several times with thickness until obtaining sufficient conductivity. How to separate the top and bottom parts electrically was not also a trivial problem.

Thus, a parameter study is conducted on g to update the design with a larger gap of g , and the results are shown in Table 1. It is seen that the gain deviation is worsened, the radiation efficiency is improved, and the resonant frequency is shifted upward with a larger g . It is mainly caused by the increased electrical size of the antenna owing to the lower gap capacitance along the arcs of the top and bottom parts, depicted in Fig. 2b. The radiation properties of the electric meander dipole antenna and magnetic loop antenna are mainly based on its wavelength. When the antenna size of the electric dipole goes higher the radiation pattern becomes more directional, leading to the increase of the maximum gain. On the other hand, when the electrical size of the loop antenna increases the maximum radiation intensity decreases along the plane of the loop thus causing decrease of the gain [24, pp. 164–168, 250–259]. Therefore, the overall gain deviation obtained from the difference between the maximum and minimum gains of the antenna becomes worsen for the larger g and results in a poorer isotropic radiation pattern. The used strip lines might offer more gap capacitance than wires, but it is found to be not enough. Thus, the design needs update with a larger g for easier and reliable copper coating while

TABLE 1. Parameter study results.

Parameter [mm]	$g = 0.2$	$g = 0.4$	$g = 1.0$
f_0 [MHz]	915	990	1,059
Gain Deviation [dB]	2.87	3.51	4.17
η_{eff} [%]	88.37	92.81	97.57

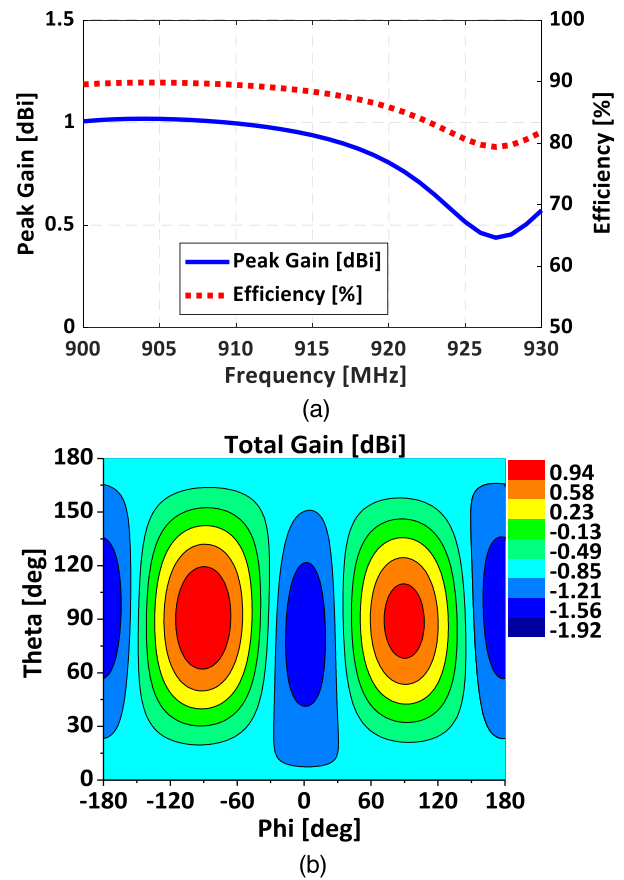


FIGURE 3. Simulated results for Figure 2. (a) Gain and radiation efficiency across the frequency. (b) Gain deviation in the entire space.

maintaining the electrical properties of the antenna including ka and gain deviation.

B. ANTENNA DESIGN UPDATE

To lower the up-shifted frequency of the proposed design with a physically larger gap of g , a vertical copper tooth structure is introduced between the top and bottom arcs, as shown in Figs. 4a and 4c. It could compensate for the decreased capacitance of the structure with a physically larger g with a series of gap capacitance from the tiny gaps (g_t , see Fig. 4c) along the arc. In addition, each metal tooth is surrounded by a plastic tube so that the top and bottom parts of the antenna could be supported with a fixed height when printed and assembled as described in Figs. 4a and 4c. The radiuses of the metal tooth r_m and plastic tube r_t in Fig. 4a are 0.5 mm and 0.7 mm, respectively.

The difference in resonant frequency between the antennas with and without the proposed vertical metal tooth is plotted in Fig. 5a. The values for g_t and g in Fig. 4c are 0.2 mm and 1.0 mm, respectively for the case of the black dashed line in Fig. 5a. It is observed that the resonant frequency is lowered from 1.059 GHz (red dotted line) to 971 MHz with the placement of the vertical tooth with the same g of 1.0 mm. Furthermore, the gain deviation is also improved

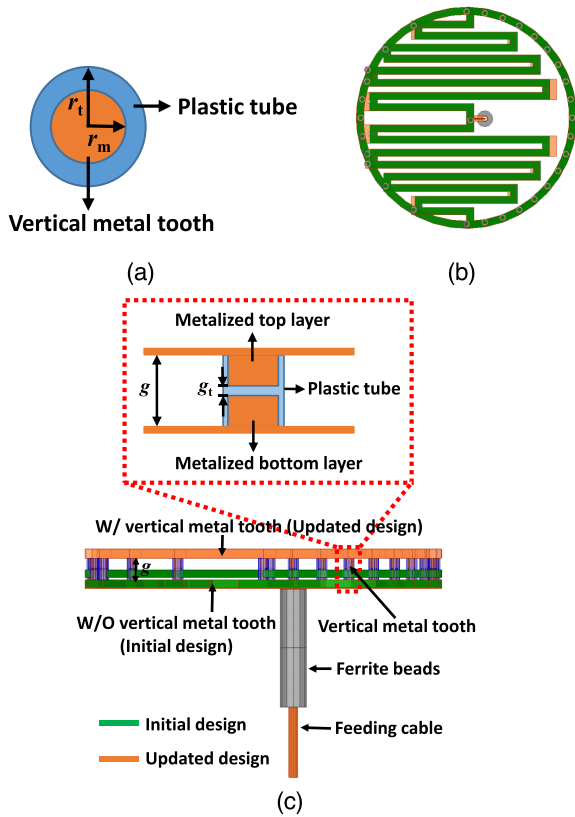


FIGURE 4. Tuned with vertical metal tooth made of copper. (a) Top view of the metal tooth with plastic tube. (b) Top view of the initial design (in green) and the updated, final design (in orange). (c) Side view of the initial design and the updated, final design.

from 4.17 dB to 3.36 dB. It is because the lowered gap capacitance could be compensated by the presence of the metal tooth along the arcs. It provides additional capacitance for the antenna and the electrical size of the antenna becomes smaller while keeping the same physically larger g . As a result, the increased maximum gain of the larger g case decreases, and the decreased minimum gain increases with the metal tooth. The change in the radiation performance of the antenna by the metal tooth is summarized in in Table 2. Consequently, we set $g = 2.2$ mm and finely tune all the design parameters. The number of metallic teeth is thirty. The increased gap, which is about ten times larger than the original gap size $g = 0.2$ mm, would make the plating process easier and reliable. In Fig. 4b, it is shown that the shape of the antenna is almost the same as in the initial design in Fig. 2, except for the slight variation in the length of the meander lines. It is thus conferred that the lowered resonant frequency in Fig. 5a and improved gain deviation are mainly caused from the vertical metal tooth. The initial and updated design are depicted in green and orange color, respectively, to show the difference in antenna configuration. The whole view of the updated, final antenna design with the magnified view of the arrangement of metal tooth is shown in Fig. 4c.

The final design parameters are given in Table 3. The resonance occurs at 918 MHz, with a maximum gain deviation

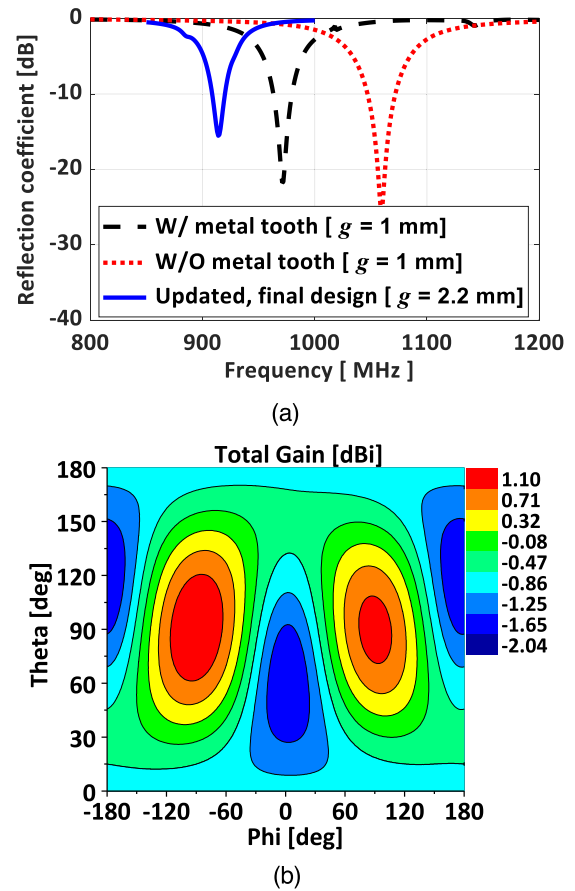


FIGURE 5. Simulated results for the final, updated antenna with the vertical metal tooth. (a) Comparison of the reflection coefficient. (b) Gain deviation of the final design.

TABLE 2. Change in radiation performance by vertical metal tooth.

Parameter [mm]	Initial design [Couldn't be built]	w/o metal tooth	w/ metal tooth
g	0.2	1.0	1.0
f_0 [MHz]	915	1059	971
Maximum gain [dBi] (@ $\theta=90^\circ, \phi=90^\circ$)	0.94	1.3	0.91
Minimum gain [dBi] (@ $\theta=90^\circ, \phi=0^\circ$)	-1.92	-2.87	-2.45
Gain Deviation [dB]	2.86	4.17	3.36

of 3.14 dB, as observed in Fig. 5b. The radiation efficiency at the resonance is 91.6 %. Consequently, the fabrication difficulties could be overcome by a little modification in the antenna geometry with minimal effect on its impedance and radiation properties.

III. ANTENNA FABRICATION AND MEASUREMENT

In general, the SLS printout seems smooth on the surface but could be porous. Any masking medium, such as lacquer, soaks in and spreads into adjacent areas during

TABLE 3. Final design parameters.

Parameter	Value	Parameter	Value	Parameter	Value
w_1	3.1	m_1	21.0	g	2.2
w_2	4.0	m_2	37.5	t	1.6
w_3	4.45	m_3	37.5	h	0.8
w_4	4.25	m_4	35.5	r	24
w_5	4.2	m_5	32.5	r_m	0.5
w_6	4.0	m_6	27.5	r_1	0.7
w_7	4.2	m_7	20.75	α	272.6
w_8	4.0	m_8	11.25		
w_9	4.6	g_1	0.2		

Note: All the units are in millimeters except α , which is in degrees.

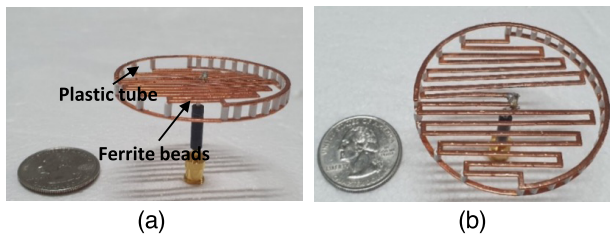


FIGURE 6. Photos of the fabricated antenna. (a) Birds view. (b) Top view.

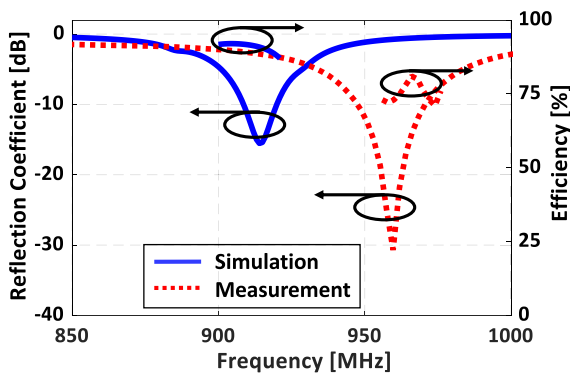


FIGURE 7. Simulated and measured reflection coefficient and efficiency.

electrochemical plating. The high-resolution SLA 3DP method could provide a smoother and less porous surface, as it forms a structure by focusing an ultraviolet laser onto a vat of photopolymer resin, while SLS uses a fine powder from many kinds of materials [25], [26]. In building the proposed antenna prototype, we first print the top and bottom layers separately using the Viper Si2 SLA printer from 3D Systems. The dielectric constant and tensile strength of the printed design are 3.5 and 56.8 MPa, respectively. They are then plated by a nano-polycrystalline copper coating technology [20], [21]. The top and bottom layers are assembled with the plastic tubes in Fig. 4 afterwards. Photos of the built antenna with ferrite beads attached to a coaxial cable are shown in Fig. 6. A quarter dollar is placed together for a size comparison.

The measured reflection coefficient and radiation efficiency are shown in Fig. 7. The simulated reflection coefficient of the final design in Fig. 5a is replotted as a solid

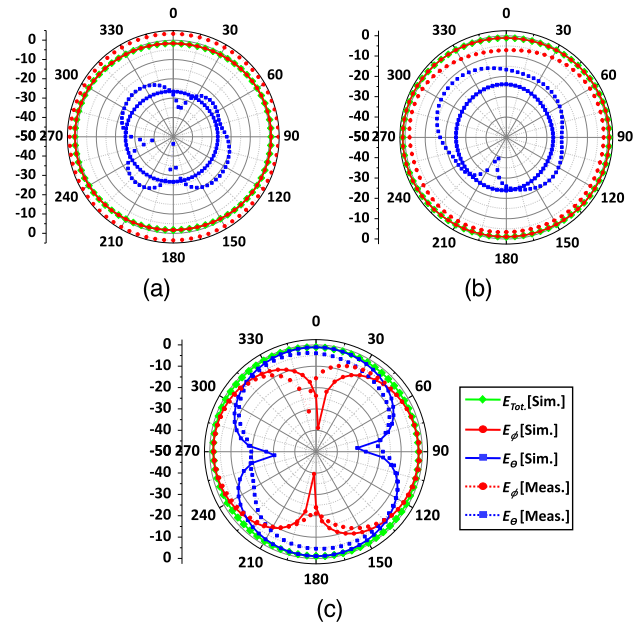


FIGURE 8. Normalized radiation pattern. (a)xy-plane. (b)yz-plane. (c) xz-plane.

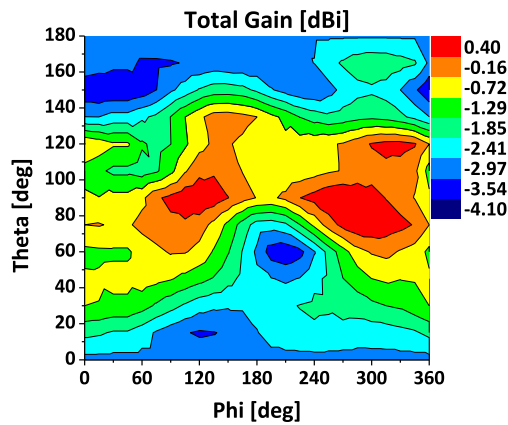
blue line for comparison. First, it can be seen that the built antenna is self-resonant, as expected from the simulation. The resonant frequency is shifted slightly upward by 43 MHz (or 4.4%) to 959 MHz, possibly due to a fabrication error caused when the two top and bottom layers are assembled. The top and bottom layers are not perfectly parallel thus the gaps by the metal tooth are a bit uneven. The possible difference in a dielectric constant of the plastic tubes in the simulation and fabrication also could be a cause. The gain and radiation pattern of the built antenna are measured in an anechoic chamber. The radiation efficiency at the measured resonance is 81 %, close enough to the simulation. A little degradation might be caused from the slightly lower conductivity of the polycrystalline copper coating than a bulk copper.

The normalized simulated and measured radiation patterns of the antenna along the elevation plane (xz - and yz -planes) and those of the antenna along the azimuthal plane (xy -plane) are plotted in Fig. 8. It is observed that the simulated and measured results are close to each other. The radiation pattern in the xy - and yz -planes is nearly uniform, whereas the xz -plane has two orthogonal omni directional E_θ and E_ϕ patterns generated by the x -directional meandered electric dipole and the z -directional magnetic dipole (or the loop formed by the arcs), respectively. The total radiated field shows a quasi-isotropic radiation. The measured gain deviation along the entire space at 959 MHz is plotted in Fig. 9. Despite it is not perfectly the same, it is seen that the measured gain distribution is much similar to the simulation in Fig. 5. The maximum and minimum gains are 0.4 dBi and -4.1 dBi, respectively; thus, a maximum gain deviation of 4.5 dB can be achieved.

Lastly, Table 4 compares the electrical sizes, the heights, the fractional bandwidth (FBW), the radiation efficiencies,

TABLE 4. Measurement result comparison of the proposed quasi-isotropic antenna and previous quasi-isotropic antennas.

Ant.	Frequency [MHz]	ka	Height	Fractional Bandwidth [%]	3DP	Efficiency [%]	Peak Gain [dBi]	Gain Deviation [dB]
[2]	888	0.41	$\lambda_0/51.97$	1.8	No	89	2.12	5.6
[3]	900 and 1800	1.16	$\lambda_0/7.6$	8.9 and 34.4	Yes	N/A	1.8	8.9 and 9.9
[4]	930	0.51	$\lambda_0/10.08$	N/A	Yes	72	0.5	N/A
[5]	2450	0.73	$\lambda_0/157.5$	0.99	No	90	1.1	3.14
[6]	2450	1.63	$\lambda_0/153.06$	20.8	No	82	2.3	5.75
[7]	2010	2.73	$\lambda_0/41.6$	18	No	N/A	N/A	12.9
[8]	2450	1.16	$\lambda_0/122.44$	11	No	N/A	1.69	6.67
This Work	959	0.48	$\lambda_0/82.32$	2.4	Yes	81	0.4	4.5

**FIGURE 9.** Measured gain deviation.

and the gain deviations of previously reported quasi-isotropic antennas with those of the antenna presented in this work. Note that all the listed values are from the measurement. It can be said that the gain deviation of the proposed antenna is competitive given its small electrical size and thin height. It also shows a good performance in terms of its compactness and radiation properties among the other quasi-isotropic antennas created using 3DP technology.

IV. CONCLUSION

In this paper, we proposed a simple yet novel configuration of an ESA showing a quasi-isotropic radiation pattern. Two layers of the meandered line with an extended arc from each arm of the dipole form an electric dipole with a loop surrounding it. The prototype of the design was 3D printed, and the proposed design was updated to be copper plated. It was observed from the measured results that the antenna is self-resonant at 959 MHz and shows a maximum gain deviation of 4.5 dB with a radiation efficiency of 81 %, which is close to the computed expectations. The electrical size ka was measured to be 0.48, with a height of $\lambda_0/82.32$.

It is worth noting that modern 3DP and copper plating technologies are able to prototype almost any complex and highly customized antenna shapes with desirable electrical properties when used with care. Herein, the initial antenna

design was tuned for its prototype fabrication using 3DP and copper plating technologies. Although this was important in the realization of this work, such the tuning procedure would be minimal if metal 3DP technology could provide highly selective printing and comparable conductivity to a bulk copper in the future. The development of a state-of-the-art hybrid 3DP technology is also ongoing and is worth to be tracked for this reason.

REFERENCES

- [1] H. F. Mathis, "A short proof that an isotropic antenna is impossible," *Proc. IRE*, vol. 39, no. 8, p. 970, 1951.
- [2] J.-H. Kim and S. Nam, "A compact quasi-isotropic antenna based on folded split ring resonators," *IEEE Antennas Wireless Propag. Lett.*, vol. 16, pp. 294–297, 2017.
- [3] Z. Su, K. Klionovski, R. M. Bilal, and A. Shamim, "A dual band additively manufactured 3-D antenna on package with near-isotropic radiation pattern," *IEEE Trans. Antennas Propag.*, vol. 66, no. 7, pp. 3295–3305, Jul. 2018.
- [4] C. Kruesi, R. Vyas, and M. Tentzeris, "Design and development of a novel 3-D cubic antenna for wireless sensor networks (WSNs) and RFID applications," *IEEE Trans. Antennas Propag.*, vol. 57, no. 10, pp. 3293–3299, Oct. 2009.
- [5] J. Ouyang, Y. M. Pan, S. Y. Zheng, and P. F. Hu, "An electrically small planar quasi-isotropic antenna," *IEEE Antennas Wireless Propag. Lett.*, vol. 17, no. 2, pp. 303–306, Feb. 2018.
- [6] C. Deng, Y. Li, Z. Zhang, and Z. Feng, "A wideband isotropic radiated planar antenna using sequential rotated L-shaped monopoles," *IEEE Trans. Antennas Propag.*, vol. 62, no. 3, pp. 1461–1464, Mar. 2014.
- [7] S. I. H. Shah, M. M. Tentzeris, and S. Lim, "Planar quasi-isotropic antenna for drone communication," *Microw. Opt. Technol. Lett.*, vol. 60, no. 5, pp. 1290–1295, May 2018.
- [8] G. Pan, Y. Li, Z. Zhang, and Z. Feng, "Isotropic radiation from a compact planar antenna using two crossed dipoles," *IEEE Antennas Wireless Propag. Lett.*, vol. 11, pp. 1338–1341, 2012.
- [9] S. Best and J. Morrow, "The effectiveness of space-filling fractal geometry in lowering resonant frequency," *IEEE Antennas Wireless Propag. Lett.*, vol. 1, pp. 112–115, 2002.
- [10] J. Gonzalez-Arbesu, S. Blanch, and J. Romeu, "Are space-filling curves efficient small antennas?" *IEEE Antennas Wireless Propag. Lett.*, vol. 2, pp. 147–150, 2003.
- [11] J. Rashed and C.-T. Tai, "A new class of resonant antennas," *IEEE Trans. Antennas Propag.*, vol. 39, no. 9, pp. 1428–1430, Sep. 1991.
- [12] H. Nakano, H. Tagami, A. Yoshizawa, and J. Yamauchi, "Shortening ratios of modified dipole antennas," *IEEE Trans. Antennas Propag.*, vol. AP-32, no. 4, pp. 385–386, Apr. 1984.
- [13] D.-O. Ko and J.-M. Woo, "Design of a small radio frequency identification tag antenna using a corrugated meander line applicable to a drug routout sensor system," *J. Electromagn. Eng. Sci.*, vol. 18, no. 1, pp. 7–12, Jan. 2018.

- [14] K. E. Kedze, H. Wang, and I. Park, "Effects of split position on the performance of a compact broadband printed dipole antenna with splitting resonators," *J. Electromagn. Eng. Sci.*, vol. 19, no. 2, pp. 115–121, Apr. 2019.
- [15] Z. Zahid, L. Qu, H.-H. Kim, and H. Kim, "Circularly polarized loop-type ground radiation antenna for IoT applications," *J. Electromagn. Eng. Sci.*, vol. 19, no. 3, pp. 153–158, Jul. 2019.
- [16] M. Kong, I.-J. Yoon, S.-H. Lee, and G. Shin, "Electrically small folded spherical helix antennas using copper strips and 3D printing technology," *Electron. Lett.*, vol. 52, no. 12, pp. 994–996, Jun. 2016.
- [17] M. Kong, G. Shin, S.-H. Lee, and I.-J. Yoon, "Investigation of 3D printed electrically small folded spherical meander wire antenna," *J. Electromagn. Eng. Sci.*, vol. 17, no. 4, pp. 228–232, Oct. 2017.
- [18] P. Nayeri, M. Liang, R. A. Sabory-Garcia, M. Tuo, F. Yang, M. Gehm, H. Xin, and A. Z. Elsherbeni, "3D printed dielectric reflectarrays: Low-cost high-gain antennas at sub-millimeter waves," *IEEE Trans. Antennas Propag.*, vol. 62, no. 4, pp. 2000–2008, Apr. 2014.
- [19] J.-C.-S. Chieh, B. Dick, S. Loui, and J. D. Rockway, "Development of a Ku-band corrugated conical horn using 3-D print technology," *IEEE Antennas Wireless Propag. Lett.*, vol. 13, pp. 201–204, 2014.
- [20] O. S. Kim, "Rapid prototyping of electrically small spherical wire antennas," *IEEE Trans. Antennas Propag.*, vol. 62, no. 7, pp. 3839–3842, Jul. 2014.
- [21] M. Kong, S.-H. Lee, G. Shin, J. Nah, and I.-J. Yoon, "Investigation of 3D printed, electrically small and thin magnetic dipole antenna," *IEEE Antennas Wireless Propag. Lett.*, vol. 17, no. 4, pp. 654–657, 2018.
- [22] P. F. Flowers, C. Reyes, S. Ye, M. J. Kim, and B. J. Wiley, "3D printing electronic components and circuits with conductive thermoplastic filament," *Additive Manuf.*, vol. 18, pp. 156–163, Dec. 2017.
- [23] W. L. Weeks, *Antenna Engineering*. New York, NY, USA: McGraw-Hill, 1968.
- [24] C. A. Balanis, *Antenna Theory: Analysis and Design*, 4th ed. New York, NY, USA: Wiley, 2016.
- [25] S. Jasvee, "Comparison of different types of 3D printing technologies," *Int. J. Sci. Res. Pub.*, vol. 8, no. 4, pp. 1–9, 2018.
- [26] K. Saloniitis, *Comprehensive Materials Processing*. Oxford, U.K.: Elsevier, 2014, pp. 19–67.



SONAPREETHA MOHAN RADHA (Student Member, IEEE) received the B.S. degree in electronics and communication engineering from Anna University, Chennai, India, in 2012, and the M.S. degree in nuclear and quantum engineering from the Korea Advanced Institute of Science and Technology, Daejeon, South Korea, in 2016. She is currently pursuing the Ph.D. degree in electrical engineering with Chungnam National University, Daejeon, South Korea. Her research interests include electrically small antennas, electromagnetic compatibility, and wireless power transfer.



GEONYEONG SHIN (Student Member, IEEE) received the B.S. and M.S. degrees in electrical engineering from Chungnam National University, Daejeon, South Korea, in 2017 and 2019, respectively, where he is currently pursuing the Ph.D. degree in electrical engineering. His research interests include antennas and theoretical methods for electromagnetics.



iversity, Daejeon, South Korea.

PANGUN PARK (Member, IEEE) received the M.S. and Ph.D. degrees in electrical engineering from the Royal Institute of Technology, Sweden, in 2007 and 2011, respectively. From 2011 to 2013, he has held a postdoctoral research position in electrical engineering and computer science from the University of California, Berkeley, CA, USA. He is currently an Assistant Professor with the Department of Radio and Information Communications Engineering, Chungnam National University, Daejeon, South Korea.



ICK-JAE YOON (Member, IEEE) received the B.S. and M.S. degrees from Yonsei University, Seoul, South Korea, in 2003 and 2005, respectively, and the Ph.D. degree from the University of Texas, Austin, TX, USA, in 2012, all in electrical engineering. He joined the faculty of Chungnam National University, Daejeon, South Korea, in 2014, where he is currently an Associate Professor with the Department of Electrical Engineering. From 2012 to 2014, he was with the Electromagnetic Systems Group, Electrical Engineering Department, Technical University of Denmark (DTU), Lyngby, Denmark, as a Postdoctoral Research Fellow and an Assistant Professor. From 2005 to 2008, he worked as a Research Engineer with the Samsung Advanced Institute of Technology of Samsung Electronics, Co., Yongin, South Korea. His current research interests include antennas, RF/microwave circuits, EMI/EMC problems from vehicles, and theoretical methods for electromagnetics. He received the H.C. Ørsted Postdoctoral Fellowship from DTU, in 2012.

...